Complete control, direct observation and study of molecular super rotors

Aleksey Korobenko[1], Alexander A. Milner[1] & Valery Milner[1]
[1] *Department of Physics & Astronomy, The University of British Columbia, Vancouver, Canada*

Extremely fast rotating molecules carrying significantly more energy in their rotation than in any other degree of freedom are known as "super rotors". It has been speculated that super rotors may exhibit a number of unique and intriguing properties. Theoretical studies showed that ultrafast molecular rotation may change the character of molecular scattering from solid surfaces[1], alter molecular trajectories in external fields[2], make super rotors surprisingly stable against collisions [3], and lead to the formation of gas vortices[4]. New ways of molecular cooling[5] and selective chemical bond breaking[6] by ultrafast spinning have been proposed. Owing to the fundamental laws of nature, bringing a large number of molecules to fast, directional and synchronous rotation is rather challenging[7–10]. As a result, only indirect evidence of super rotors has been reported to date[11–13]. Here we demonstrate the first controlled creation, direct observation and study of molecular super rotors. Using intense laser pulses tailored to produce an "optical centrifuge"[8, 11], we spin different species, from lighter H_2 to heavier O_2 and CO_2, to ultrafast uni-directional rotation with variable angular velocity. We increase the molecular rotational energy by more than two orders of magnitude and follow the evolution of super rotors with femtosecond time resolution. This allows us to observe the stretching of chemical bonds due to the centrifugal distortion, and the increased stability of rotational coherence at high angular momentum. We demonstrate that molecular super rotors can be created in dense samples under normal conditions where many-body effects, intermolecular collisions and chemical reactions can be readily explored. Our results shed new light on the fundamental correspondence between the classical state of motion and its quantum wave packet representation. As virtually all molecules are amenable to laser spinning, we anticipate this work to stimulate new studies of molecular dynamics and interactions at previously inaccessible limits.

PACS numbers:

Control of molecular rotation has been used for steering chemical reactions in gases[14] and at gas-surface interfaces[15, 16], for imaging individual molecular orbitals[17] and generating extreme ultraviolet radiation[18, 19], for deflecting molecular beams[20] and separating molecular isotopes[21]. Despite the growing list of applications, currently available methods of exciting molecular rotation exhibit relatively low degree of control. Rotational excitation based on collisions with vibrationally hot molecules[7] or impulsive excitation by ultrashort laser pulses[22] is inefficient and lacks selectivity with respect to both the final direction and speed of molecular rotation. Although sequences of pulses have been successfully used for selective[23–25] and directional[26–29] rotational excitation, the range of accessible angular velocities has been limited by the molecular breakdown in strong laser fields required for reaching the states of high angular momentum.

The appeal of creating such super rotor states by refining the degree of rotational control has resulted in a number of theoretical proposals[8–10, 30], in which molecules are exposed to longer non-ionizing laser pulses. Key to all these proposals is the idea of guiding the molecules up the "ladder" of rotational levels "step-by-step" instead of exerting an indiscriminate ultrashort rotational kick. Molecular spinning with an "optical centrifuge", suggested by Karczmarek *et. al.* and implemented in this work, is achieved by forcing the molecules to rotate together with a rotating polarization of a laser pulse[8]. The final speed of rotation is determined by the spectral bandwidth of the laser pulse and may exceed 10^{13} revolutions per second. To make O_2 molecules rotate primarily with this speed in thermal equilibrium, the gas temperature would have to be risen to above 50,000 Kelvin.

Since the original proposal[8], an optical centrifuge has been implemented by two experimental groups. In the pioneering work by Villeneuve *et. al.*, dissociation of chlorine molecules exposed to the centrifuge field has been attributed to the breaking of the Cl-Cl bond which could not withstand the extremely high spinning rates[11]. More recently, Yuan *et. al.* observed rotational and translational heating in the ensembles of CO_2 and N_2O molecules and associated it with the collisional relaxation of the centrifuged species[12, 13]. In both cases, an incoherent secondary process (i.e. dissociation and multiple collisions) has been used for indirect identification of the formation of super rotors whose most unique property - their synchronous uni-directional rotation, remained hidden. In this work, we *control* the direction and final speed of molecular rotation and employ a *coherent* detection technique to probe it directly. We follow the molecules as they spin up inside the centrifuge and, after the molecules are released from the centrifuge, analyze their free evolution in unprecedented range of rotational angular momentum, $J \lesssim 300$ for CO_2 and $J \lesssim 100$ for O_2. High spectral resolution of our detection enables us to reveal the relatively narrow width of the created rotational distribution indicating high selectivity of centrifuge spinning.

Following the recipe of Karczmarek *et. al.*[8], we cre-

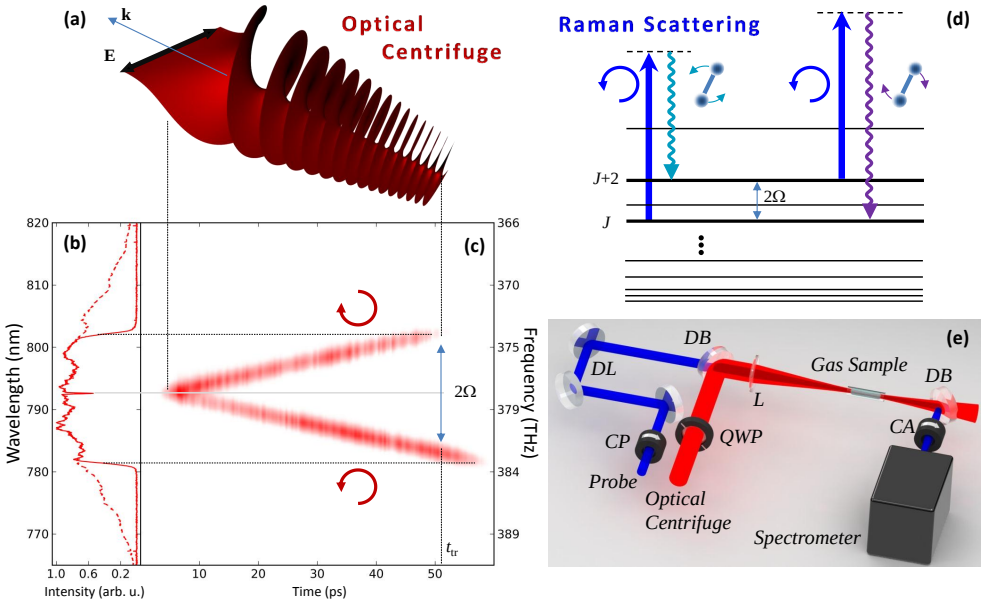

FIG. 1: **a,** Illustration of an optical centrifuge field propagating in the direction **k**. The vector of linear polarization **E** undergoes an accelerated rotation, completing about 125 turns during a 50 ps centrifuge pulse and reaching frequencies on the order of 10^{13} Hz (for clarity, much lower angular acceleration is shown in the picture above). A laser-induced dipole force keeps the molecules aligned with **E**, accelerating them to the ultra high rotational velocities of a "super rotor". The centrifuge is truncated at time $t_{\rm tr}$ in order to terminate the acceleration and release the molecules with a well defined final angular frequency Ω. Experimentally measured frequency spectra of the centrifuge pulse before and after truncation are shown in panel **b** by dashed and solid red lines, respectively. To create the centrifuge, we split an ultrashort laser pulse at the center of its spectrum (horizontal grey line) with a home built pulse shaper. The shaper is used to chirp the two spectral parts, sweeping their instantaneous frequencies in opposite directions, as confirmed by the experimentally recorded time-frequency spectrograms shown in panel **c** (tilted red traces). Rotating the polarization plane of a centrifuge is achieved by polarizing the two spectral components with an opposite sense of circular polarization (red circles). The instantaneous frequency difference, $2\Omega(t)$, between the left and right circularly polarized components grows in time, resulting in a gradual increase of the centrifuge angular frequency $\Omega(t)$. **d**, Coherent Raman scattering is employed to determine the speed and direction of molecular rotation. Weak probe pulses (blue lines) of circular polarization (blue circle) are scattered off the centrifuge-induced rotational coherence between the quantum states separated by $\Delta J = \pm 2$. The magnitude of the Raman frequency shift equals twice the rotation frequency, while its sign reflects the direction of molecular rotation. **e,** Experimental set up. Centrifuge pulses (red) are combined with a probe beam (blue) on a dichroic beamsplitter (DB) and focused into a windowless gas cell by a 1 m-focal length lens (L) to a beam diameter of 120 μm (full width at half maximum). Control of the spinning direction is executed by a quarter-wave plate (QWP). Probe pulses are polarized with a circular polarizer (CP), delayed with a delay line (DL), filtered out with a second dichroic beamsplitter and a circular analyzer (CA). Probe spectrum is recorded with a 0.6 nm-resolution spectrometer.

ate an optical centrifuge by generating a linearly polarized field with the polarization plane rotating along the propagation axis as illustrated in Fig.1**a**. Accurate experimental characterization of the centrifuge field shows that the centrifuge angular frequency gradually increases from 0 to 10 THz in the course of about 100 ps (Fig.1**b**,**c**). Truncating the centrifuge at a predetermined time $t_{\rm tr}$ enables us to set the final speed of molecular rotation Ω.

The centrifuge pulse is focused into a windowless gas cell with a constant flow of various gases at room temperature and atmospheric pressure (Fig.1**e**). Special care is taken to avoid ionization and plasma breakdown by limiting the peak intensity of the excitation field to below 5×10^{12} W/cm^2. Increasing the excitation strength above this limit resulted in strong ionization and disappearance of super rotors. Key to this work is the use of coherent Raman scattering of probe light from the rotating molecules. Quantum mechanically, synchronous molecular rotation corresponds to a superposition of a few rotational quantum states - a "rotational wave packet", with an average frequency separation matching the frequency of the classical rotation. Owing to the wave packet coherence, the probe spectrum acquires two frequency sidebands, known as Stokes and anti-Stokes components shifted down and up from the central probe frequency, respectively (Fig.1 **d**). The frequency shift, which can also be viewed as a result of the rotational Doppler effect[29], equals twice the rotation frequency of the molecules and can therefore serve as an unambiguous quantitative measure of molecular spinning.

In Figure 2 **a** we show the spectrum of linearly polarized probe pulses passing the centrifuged volume of ambient air. The appearance of both Stokes and anti-Stokes sidebands at 401 and 393 nm, respectively, indi-

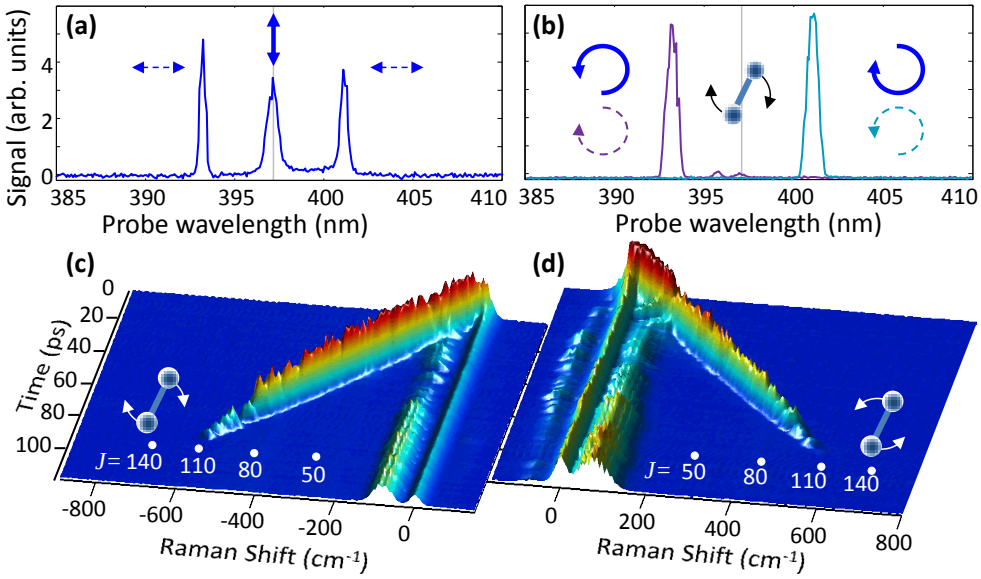

FIG. 2: Raman spectrum of a centrifuged volume of ambient air with linearly (**a**) and circularly (**b**) polarized probe pulses arriving 36 ps after the leading edge of the centrifuge pulse. The spectrum, initially comprised of a single narrow peak at 397 nm (grey line), develops two sidebands indicating coherent Stokes and anti-Stokes scattering from the rotating molecules. In plot **b**, circular polarization of the two Raman sidebands (dashed circles) is opposite to probe polarization (solid circles). Whether the frequency shift is negative (right cyan sideband) or positive (left purple sideband) depends on the relative handedness of probe polarization and centrifuge-induced molecular rotation. Time-dependent Raman shifts from the centrifuged oxygen molecules are shown in panels **c** and **d** for the case of clockwise and counter-clockwise centrifuge spinning, respectively, and a fixed counter-clockwise probe polarization. As the molecules spend longer time in the centrifuge, the observed Raman frequency shift increases, providing a direct evidence of accelerated molecular rotation in one well defined direction. From the frequency shift we extract the rotational quantum number J indicated by white labeled dots. Remarkably, by the end of a 100 ps centrifuge pulse O_2 super rotors reach rotational levels as high as $J \approx 100$. On both plots, we note a few additional features with much smaller and time independent Raman shifts, which are attributed to the complex molecular behavior inside the centrifuge.

cates coherent molecular rotation. For a circularly polarized probe, however, only one sideband is allowed by the law of conservation of angular momentum. In this case, the sign of the frequency shift is dictated by the relative direction of the molecular rotation and probe electric field. Stokes peak indicates molecular rotation in the same direction as probe polarization, whereas molecular rotation of the opposite sense results in anti-Stokes frequency shifting. As demonstrated in Fig.2 **b**, making the probe polarization circular indeed leaves only one sideband in the recorded spectra, confirming the anticipated directionality of molecular rotation.

Delaying the arrival time of probe pulses with respect to the beginning of the centrifuge results in the growing frequency shift of the Raman line, in agreement with the expected increase of the induced spinning rate. In Figure 2 **c**,**d**, the rotational Raman shift in oxygen is plotted as a function of time a molecule spent in the centrifuge. The two plots correspond to two opposite senses of the centrifuge rotation and demonstrate the successful molecular spinning in both directions. Conversion of the detected Raman shift to the rotational quantum number J of O_2 is shown with white labeled dots. One can see that the centrifuge is indeed capable of creating molecular super rotors by accessing an amazingly broad range of final angular momenta ($J > 100$), more than an order of magnitude above the peak of the room-temperature distribution at $J = 8$. From the observed Raman spectrum, we can evaluate the relatively narrow width of the excited rotational wave packet, $\Delta J \approx 7$. This important feature of a super rotor state offers a unique opportunity to study the rotation of a quantum object at its classical limit, when the quantization of rotational energy is not apparent on the time scale of one rotational period.

One may wonder as to why does the Raman signal disappear at the end of the centrifuge pulse at around 100 ps (Fig.2 **c**,**d**). After all, the molecules should not stop spinning when they escape the centrifuge. Neither should oxygen dissociate before reaching much higher rotational states estimated at $J \approx 230$. We attribute the loss of the signal to the leakage of molecules from the weakening centrifuge at the end of the spinning process. Because of such uncontrolled leakage, molecules start their free rotation with a large spread of initial phases, lowering the total rotational coherence of the ensemble and, therefore, the amplitude of coherent Raman response. To control both the speed and the phase spread of molecular rotation, we truncate the centrifuge pulse and release

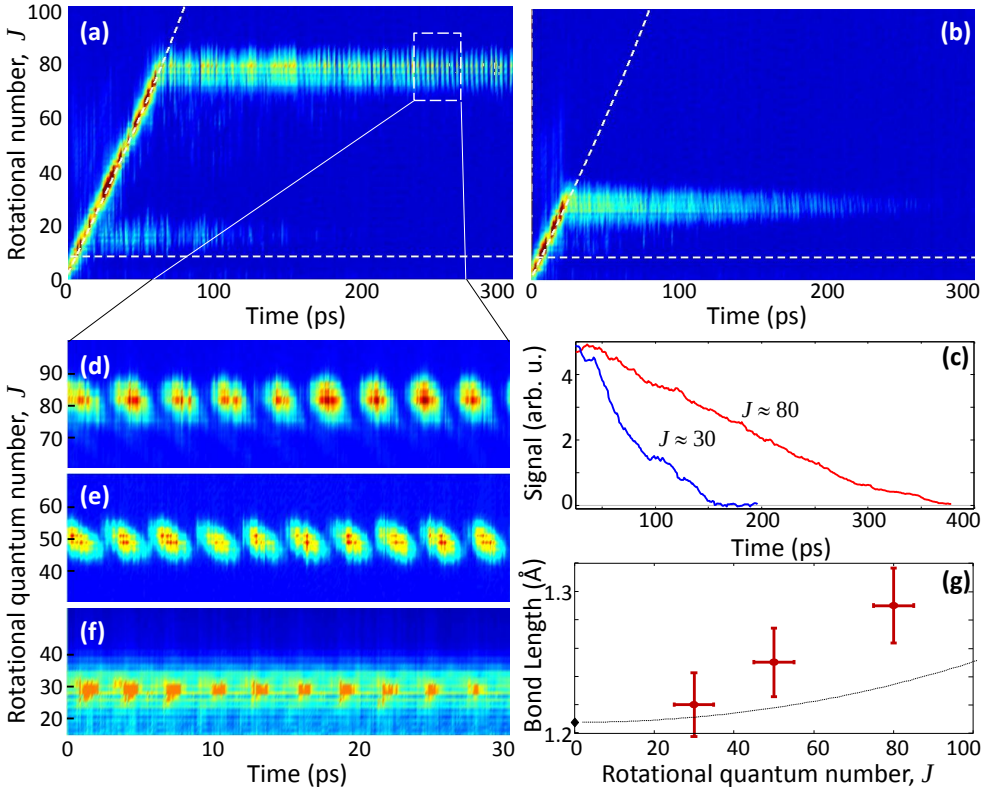

FIG. 3: **a,b** Selective centrifuge spinning of oxygen to $J = 80$ and $J = 30$, respectively. Raman frequency shift is measured as a function of time for an optical centrifuge truncated at $t = 64$ ps (**a**) and $t = 24$ ps (**b**). Until the time of release, molecular rotation follows the angular frequency of the centrifuge, which is determined (with no fitting parameters) from the experimental time-frequency spectrograms described in Fig.1 and shown here with dashed tilted lines. A horizontal Raman trace originating at the end of the centrifuge pulse indicates free rotation of molecular super rotors with a well defined ultra high angular momentum. For comparison, dashed horizontal lines mark the most populated rotational state of O_2 at room temperature, $J = 8$. It is evident from plots **a** and **b** that the decay of coherent molecular rotation is slower for molecules spinning with higher angular momentum. This notable result is summarized in plot **c**, where we show the averaged (over 50 ps) Raman signal as a function of the time elapsed since the release from the centrifuge. Zooming in the time window between 230 and 260 ps reveals periodic oscillations shown in panels **d-f** and representative of the coherent dynamics of rotational quantum wave packets. The oscillation period depends on the molecular moment of inertia and hence the distance between the two oxygen nuclei. Fourier analysis of the observed oscillations enables us to examine the bond length of a molecule as a function of its angular momentum (panel **g**). We find that the centrifugal force stretches the chemical bond to 1.22 Å, 1.25 Åand 1.29 Åfor $J = 30$, 50 and 80, respectively, or up to 10% from its equilibrium value indicated by black diamond. Theoretical predictions based on a simple model described by the rotating Morse potential are plotted with dashed line. The apparent disagreement calls for a refined analysis of molecular potentials at such high levels of angular momenta.

the molecules before the laser field becomes too weak to trap them. As shown in Fig.3, molecules released in a controlled way keep generating coherent Raman signal, which confirms their free super rotation. The data in panels **a** and **b** correspond to the truncated centrifuge which spun O_2 molecules from around $J = 8$ to $J \approx 80$ and $J \approx 30$, respectively.

We note that the strength of coherent Raman scattering decays on the scale of a few hundred picoseconds, comparable with the average time between collisions estimated at ≈ 150 ps. This suggests an extremely fragile nature of coherent rotational wave packets, in sharp contrast to the previously observed long life time of incoherent rotational excitation. Even though the molecules may not lose their rotational energy easily, the phase of their rotation is scrambled rather quickly. For the first time, we observe the anticipated increase of rotational stability with increasing angular momentum, evident from the slower decay of rotational coherence at higher spinning rates of a super rotor, as shown in Figure 3 **c**.

We also notice a fine structure in the dynamics of the freely rotating centrifuged molecules. Zooming in with higher time resolution reveals periodic oscillations of the induced rotational wave packet, shown in Figure 3 **d-f** for three different values of the angular momentum. Periodic structure is the distinctive signature of a discrete energy spectrum of a quantum rotator. The oscillation period T depends on the reduced mass of a molecule, μ, and the

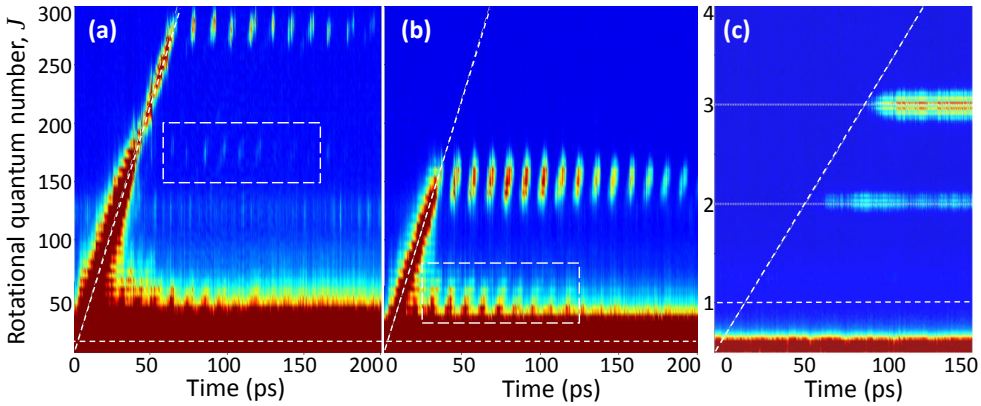

FIG. 4: Centrifuge spinning of CO_2 and H_2 molecules. Owing to a much bigger moment of inertia than oxygen, carbon dioxide can be spun to much higher rotational states. In **a** and **b**, super rotor wave packets centered at $J \approx 275$ and $J \approx 150$, respectively, are generated with truncated centrifuge pulses and their field free periodic dynamics are followed in time. Dashed rectangles emphasize the complexity of the centrifuge process by highlighting unexpected periodic signals from molecules leaking through a "hole" in an imperfect centrifuge either high up the rotational "ladder" (left) or close to its lower end (right). The result of applying an optical centrifuge to molecular hydrogen is shown in panel **c**. As anticipated, continuous centrifuge spinning translates here into a series of discrete steps between largely separated rotational levels of much lighter H_2 molecule. Bridging the gap to higher rotational states, $J \geq 4$, would require much broader laser bandwidth. As in Fig.3, dashed lines represent experimentally determined angular frequency of the centrifuge, and the most populated rotational level at room temperature.

distance between the two atoms R as $T = \frac{\pi}{2\hbar}\mu R^2$, where $\hbar$ is the reduced Planck constant. Under normal conditions, oxygen nuclei inside O_2 are separated by 1.21 Å. However, fast molecular rotation pulls the atoms apart. The effect of lengthening the molecular bond, known as the centrifugal distortion, slows down the free rotation and increases the oscillation period. The ability to accurately measure rotational bond stretching for a broad range of rotational states offers a new opportunity to study complex molecular motion in the limit of ultra-fast rotation. In panel **g** of Fig.3, we compare the experimentally retrieved inter-nuclear distances for J=30, 50 and 80 with a simple model of a rotating Morse oscillator, which clearly fails to describe molecular bond stretching at this limit.

Because it is based on a non-resonant molecular polarizability, the method of controlled centrifuge spinning can be applied to virtually any molecular species. In addition to O_2 , we have successfully produced and observed N_2 and CO_2 super rotors. Coherent uni-directional rotation of carbon dioxide excited to $J \approx 275$ and $J \approx 150$ is presented in Figure 4 **a** and **b**, respectively. The figure also illustrates the complexity of the laser induced dynamics, identified by the appearance of coherent oscillatory Raman response at lower J values. Applying the centrifuge to much lighter molecules demonstrates the quantum limit of the technique, which is reached when the spectral bandwidth of the laser pulse becomes comparable to the frequency separation of the rotational quantum states. Figure 4 **c** illustrates this limitation for the case of H_2 molecules. Instead of a continuous rotational acceleration, our centrifuge executes only two discrete steps corresponding to $J = 0 \rightarrow J = 2$ transition in parahydrogen and $J = 1 \rightarrow J = 3$ transition in orthohydrogen.

Control of molecular rotation in extremely broad range of angular frequencies reported in this work paves the way for a new exploration of fundamental physics and chemistry at previously inaccessible limits. Centrifugal bond stretching and slow rotational de-phasing at ultra high angular momenta, demonstrated here, are only two examples of the utility of controlled molecular spinning. Exciting new tests of kinematic, electrical, magnetic, acoustic, optical and reactive properties of molecular super rotors are within reach.

This work has been supported by the CFI, BCKDF and NSERC. We thank Gilad Hurvitz and Sergey Zhdanovich for their help with the experimental setup. We gratefully acknowledge stimulating discussions with John Hepburn, Ilya Averbukh and Yehiam Prior.

[1] Y. Khodorkovsky, J. R. Manson, and I. Sh. Averbukh, Phys. Rev. A **84**, 053420 (2011).
[2] E. Gershnabel and I. Sh. Averbukh, Phys. Rev. Lett. **104**, 153001 (2010).
[3] K. Tilford, M. Hoster, P. M. Florian, and R. C. Forrey, Phys. Rev. A **69**, 052705 (2004).
[4] U. Steinitz, Y. Prior, and I. Sh. Averbukh, Phys. Rev. Lett. **109**, 033001 (2012).
[5] R. C. Forrey, Phys. Rev. A **66**, 023411 (2002).
[6] R. Hasbani, B. Ostojic, P. R. Bunker, and M. Y. Ivanov,

J. Chem. Phys. **116**, 10636 (2002).
[7] A. S. Mullin, C. A. Michaels, and G. W. Flynn, J. Chem. Phys. **102**, 6032 (1995).
[8] J. Karczmarek, J. Wright, P. Corkum, and M. Ivanov, Phys. Rev. Lett. **82**, 3420 (1999).
[9] J. Li, J. T. Bahns, and W. C. Stwalley, J. Chem. Phys. **112**, 6255 (2000).
[10] J. P. Cryan, J. M. Glownia, D. W. Broege, Y. Ma, and P. H. Bucksbaum, Phys. Rev. X **1**, 011002 (2011).
[11] D. M. Villeneuve, S. A. Aseyev, P. Dietrich, M. Spanner, M. Y. Ivanov, and P. B. Corkum, Phys. Rev. Lett. **85**, 542 (2000).
[12] L. Yuan, S. W. Teitelbaum, A. Robinson, and A. S. Mullin, PNAS **108**, 6872 (2011).
[13] L. Yuan, C. Toro, M. Bell, and A. S. Mullin, Faraday Discussions **150**, 101 (2011).
[14] R. N. Zare, Science **279**, 1875 (1998).
[15] E. W. Kuipers, M. G. Tenner, A. W. Kleyn, and S. Stolte, Nature **334**, 420 (1988).
[16] D. Shreenivas, A. Lee, N. Walter, D. Sampayo, S. Bennett, and T. Seideman, J. Phys. Chem. A **114**, 5674 (2010).
[17] P. B. Corkum and F. Krausz, Nat. Phys. **3**, 381 (2007).
[18] J. Itatani, D. Zeidler, J. Levesque, M. Spanner, D. M. Villeneuve, and P. B. Corkum, Phys. Rev. Lett. **94**, 123902 (2005).
[19] N. Wagner, X. Zhou, R. Lock, W. Li, A. Wüest, M. Murnane, and H. Kapteyn, Phys. Rev. A **76**, 061403 (2007).
[20] S. M. Purcell and P. F. Barker, Phys. Rev. Lett. **103**, 153001 (2009).
[21] S. Fleischer, I. Sh. Averbukh, and Y. Prior, Phys. Rev. A **74**, 041403 (2006).
[22] T. Seideman, J. Chem. Phys. **115**, 5965 (2001).
[23] M. Renard, E. Hertz, B. Lavorel, and O. Faucher, Phys. Rev. A **69**, 043401 (2004).
[24] S. Fleischer, I. Sh. Averbukh, and Y. Prior, Phys. Rev. Lett. **99**, 093002 (2007).
[25] S. Zhdanovich, C. Bloomquist, J. Floß, I. Sh. Averbukh, J. W. Hepburn, and V. Milner, Phys. Rev. Lett. **109**, 043003 (2012).
[26] S. Fleischer, Y. Khodorkovsky, Y. Prior, and I. Sh. Averbukh, New J. Phys. **11**, 105039 (2009).
[27] K. Kitano, H. Hasegawa, and Y. Ohshima, Phys. Rev. Lett. **103**, 223002 (2009).
[28] S. Zhdanovich, A. A. Milner, C. Bloomquist, J. Flo, I. Sh. Averbukh, J. W. Hepburn, and V. Milner, Phys. Rev. Lett. **107**, 243004 (2011).
[29] O. Korech, U. Steinitz, R. J. Gordon, I. Sh. Averbukh, and Y. Prior, in *XVIIIth International Conference on Ultrafast Phenomena* (EPJ Web of Conferences, 2013), vol. 41, p. 02020; arXiv:1303.6758.
[30] N. V. Vitanov and B. Girard, Phys. Rev. A **69**, 033409 (2004).